A wearable flexible battery using human body temperature differences

Gao Shuyan[1*], $ZhangZihan^2$, $ZhangYan^3$, $ZhouJunming^4$

June 21, 2023

1 School of Energy and Power Engineering, Chongqing University, Chongqing 400044, China
2 School of Energy and Power Engineering, Chongqing University, Chongqing 400044, China
3 School of Civil Engineering, Chongqing University, Chongqing 400044, China
4 School of Physics, Nankai University, Tianjin 300071, China
* Correspondence: 20203109@stu.cqu.edu.cn; Tel.:+86-15890570553

1 Abstract

Ionic battery materials are widely used in wearable devices, especially ionic gel materials. In the face of a variety of ionic thermoelectric materials, it is a key issue to select the appropriate thermoelectric ones for different artificial heart power supply needs. In this study, it is aimed to establish a database of ionic thermoelectric materials for existing wearable devices, compare the battery performance under different boundary conditions and different materials based on the physical model of the battery, and select the optimal battery material suitable for an artificial heart. 72 kinds of ionic thermoelectric materials were identified through a literature review. The properties of ionic thermoelectric materials were comprehensively considered from the aspects of the Seebeck coefficient, electric conductivity, and power factor. The materials were determined by a thermoelectric figure of merit (ZT). The physical model of the battery was established by Solidworks. The three-dimensional physical field of thermoelectric materials was analyzed by COMSOL, so as to clarify the temperature and potential change characteristics of thermoelectric materials under different boundary conditions and different material types. Finally, the thermoelectric material with the largest electric potential energy was selected. Under a constant temperature boundary condition of 33 ℃ and 5 ℃, the maximum potential produced was 23.21 mV. By changing the materials and keeping other conditions unchanged, it was found that the potential generated by the six ion gel materials is mostly mV.

Keywords:ionic battery,ionic thermoelectric material,wearable device.

2 Project Background

Energy conversion based on thermoelectric properties has recently attracted much attention due to its fundamental and applied perspectives. Thermoelectric Generation (TEG) provides heat loss recovery of thermodynamic units for power production. The principle of TEG is the Seebeck effect. The Seebeck effect is the production of an electromotive force and consequently an electric current in a loop of material consisting of at least two dissimilar conductors when two junctions are maintained at different temperatures[1].

The heat loss of the human body can be employed for thermoelectric power production. The human body is a relatively constant ideal heat source: the heat power lost to the environment by the entire body surface is about 60-180 W. If TEG technology is used to convert 1% of the human body heat dissipation into electrical energy, the power generation power reaches 0.6-1.8W[2].

The IDC Quarterly Global Wearables Tracker shows that wearable device usage is increasing year by year worldwide. For wrist-worn devices, this wearable battery can be directly used as a bracelet to connect to the device: for ear devices, it can be used as a power bank to charge the device when it is low on power[3]. In view of the current widespread short battery life defects in wearable devices, this can solve the problem of frequent battery replacement and device charging when there is no power supply nearby, reduce the battery cost to people who rely on cochlear and other hearing aids, and achieve an autonomous supply, which is more favoured by the public. At the same time, this battery uses temperature differences between the human body and the environment, focuses on environmental protection issues, makes full use of the energy emitted by the human body, and will hopefully replace the disposable battery in equipment[4], so as to actively respond to national policies, achieve energy conservation and emission reduction, and conform to the direction of future energy development.

3 Division of roles & responsibilities

NAME	Role	RESPONSIBILITY
Zhang Zihan	Resource investigator	Data collecting and analysis
Zhang Yan	Leader	Modeling and simulation
Gao Shuyan	Spokesperson	Modeling
Zhou Junming	Teamworker	Simulation

4 Challenges & Solutions

4.1 Data

At the beginning of the project, we planned to implement data collection through Python crawlers. Due to our limited capacity and the quite short time available in the work process, we decided to collect relevant data on thermoelectric materials by consulting a wide range of literature. Although the collection process was slow and extensive, we managed to collect 72 sets of data. Among the data we collected, the parameters of most materials were not complete. For example, some materials had a Seebeck coefficient but no thermal conductivity coefficient, which meant that the ZT value of some materials could not be obtained. It was thus decided to obtain the missing parameter by averaging the parameters of other materials or by analogy.

4.2 Modeling

We used Solidworks to deduce the structure of the physical model. Initially, we did not know how to determine its size in a reasonable way. In that case, we consulted references, took flexibility into consideration, and eventually determined the size of the electrodes and galvanic couple to be 2cm by 2cm by 0.5cm and a cube with sides of 2cm, respectively. When choosing the electrode material, there was a difficult choice to be made as to brass or copper. Given that the conductivity of copper has better qualities, we chose copper to be the electrode material.

4.3 Simulation

During the simulation, the potential difference between the two ends of the battery was found to be too small to meet the power supply demand of the artificial heart. According to the size and material density of the battery, the weight of this model is 0.4 g. Taking the weight of a short sleeve in summer (100 g) as a reference, nearly 500 basic units of the battery need to be connected in series. However, this is limited by the computational power of the PC. To solve this problem, we selected the structure of two basic units in series to obtain the potential difference generated by the battery under unit mass and then calculated the potential difference generated under actual size. Here, the similarity principle of experimental design is referred to.

5 Contributions & limitations

5.1 Data

72 sets of data were collected including 16 different primary materials as substrates, loading different ionic solutions with different treatments, as shown in Figures 1 and 2. Through data visualization (Figure.3) we can see that the ionic conductivity of ionic thermoelectric materials is not directly proportional to the Seebeck coefficient. In most cases, the Seebeck coefficient is relatively small. Thus, when constructing the battery model, choosing materials that have relatively a high Seebeck coefficient and also high ionic conductivity is a key point. Among the collected data, 7 groups of data (figure 4) were selected for simulation. The reason why they were chosen is that, compared with other values of materials, the Seebeck coefficient, ionic conductivity, and thermal power of these 7 sets are relatively higher, thus allowing a higher battery voltage to be obtained.

Primary Material	Treatment/Device Fabrica..	Additives/Dopants	Eletrical Conductivity	Seebeck Coefficient	Power Factor
Cellulose acetate	Bar-coating	SWCNT(90wt%)	873.00	45.5	1.41
F8bpy	Solution mixing	SWNT(90%)	290.00	46.3	62.30
Nafion	Simple mixing	FWNT(30wt%)	12.50	27	1.00
P3HT	In situ chemical polymeriz..	SWNT(60%)	2760.00	31.1	267.00
	Solution mixing	MWNT(5%)	576.00	29.1	49.00
PANI	Cryogenic grinding	MWNT(30%)	1.59	26	0.11
	In suti chemical polymerization	CNT(40%)	17.10	10	0.17
		CNT(94%)	2012.00	37	273.00
		GNP(30%)	29.00	28.7	2.40
			604.00	14.5	12.70
		GNP(57%)	59.00	33	Null
		MWNT(44%)	40.35	23.3	Null
		MWNT(94%)	14.10	79.8	Null
	Layer-by-layer	DWNT&GNP	1080.00	130	1825.00
	Mechanically grinding	GNP(50%)	123.00	33	14.00
	Solid-state grinding and d..	GNP(45%)	850.00	15	19.00
	Solution mixing	DWNT(30%)	610.00	61	220.00
		S/DWNT(50%)	29.95	119	42.00
		SWNT(64%)	769.00	47.8	176.00
PC	Melt-mixing	MENT-COOH/CBT(2.5wt%)	5.00	13.55	7.6×10-6
PDMS	Solution mixing and curing	MWCNTs(10wt%)	Null	10.4	Null
PEDOT	Hybrid films prepared via ..	Bi2Te3	Null	185	1350.00
	In suti polymerization	rGO(16%)	50.80	31.8	5.20
PEDOT:PSS	Null	SWCNT	1.35×10^3	Null	160.00
	Dispersion,chemical post..	VA-CNTF;DMSO;EG	1131.00	1131	92.00
	Solution mixing,ultra-..	Bi0.5Sb1.5Te3;PVA	23.00	144	47.70
	chemical oxidation polym..	Null	570.40	17.5	19.00
	Dilution-filteration	SWNT(50%)	900.00	30	83.90
	Dual-stabilizer	DWNT(40%)	960.00	70	500.00
	Hot-pressing	CNT(50%)	2350.00	49.3	572.00
	IL and PEDOT:PSS stirred ..	LiTFSI ionic liquid(IL)	1000.00	35	75.00

Figure 1: Data

5.2 Modeling

The physical model consists of electrodes and a galvanic couple. The size of the electrodes is 2cm by 2cm by 0.5cm. The galvanic couple is a cube with sides of 2cm. We assumed the upper and lower

Primary Material	Treatment/Device Fabrica..	Additives/Dopants	Eletrical Conductivity	Seebeck Coefficient	Power Factor
PEDOT:PSS	Mixing in solution	CuCl2	Null	18200	1700.00
	Nanosheet powder disper..	SnSe0.97Te0.03 nanosheet	18.00	90	14.73
	Post-treatment	DWNT(20%)	780.00	43.7	151.00
	Preparation of thin film a..	Formic Acid	1900.00	20.6	3.00
	Road-coating	MWNT(2%)	74.00	18.5	Null
	Solution coated onto paper	DMSO;EG	0.20	30.6	6.41
	Solution mixing	SWNT(6.70%)	1350.00	59	464.00
		SWNT(35%)	400.00	25	25.00
		SWNT(60%)	1350.00	41	160.00
	Spin-coated onto PDMS then annealed; application of tensile strain	DMSO	891.00	21.76	Null
		EG	942.00	19.1	Null
		H2SO4	Null	18.32	61.18
		MeOH	1200.00	18.7	35.10
		PEG	882.00	19.95	47.20
	Stretching;treated with D..	Xylitol;DMSO or water	1155.00	18.1	80.60
	Two-step spin casting	SWNT	241.00	38.9	21.10
	Vacuum filteration	GNP(3%)	1283.50	22	38.60
		SWNT(60%)	600.00	44.3	105.00
	Wet-chemical route	rGO(3%)	1160.00	17	32.60
	Wet-spinning and post-tr..	SWNT(15%)	0.06	Null	1200.00
PEI	Solution mixing and vacuu..	SWNT(10vol%)	200.00	43	0.04
PEI/NaBH4	Simple mixing	SWNT	20.00	-80	128.00
PPy	In suti chemical polimeriz..	SWNT(60%)	399.00	22.2	19.70
	In suti chemical polymerization	GNPs(40%)	101.68	31.74	10.24
		rGO(50%)	75.10	33.8	8.57
		rGO(66.67%)	41.30	27	3.01
	Solution mixing	SWNT(60%)	300.00	26.9	21.70
PS	Simlpe mixing	CNT(75wt%)	2.10	57	0.15
PSB	Physical and solution mixi..	graphite(80%)	231.00	21	10.20
PVAc	Segregated network	CNTs(20wt%)	48.00	80	30.70
		DNCNT:TCPP(12wt%)	71.09	78	42.80

Figure 2: Data

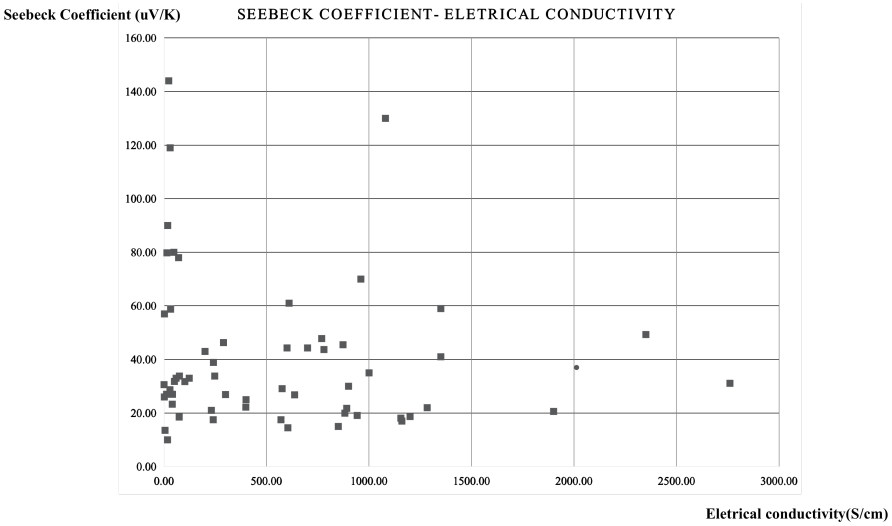

Figure 3: Seebeck coefficient-Electrical conductivity

Materials for modeling					
Primary Material	Additives/Dopants	Treatment/Device Fabrication	Seebeck Coefficient (uV/k)	Eletrical Conductivity (S/cm)	Power Factor ($uW \cdot m/k^2$)
PEDOT:PSS	CuCl2	Mixing in solution	18200	———	1700
PEDOT	Bi_2Te_3	Hybrid films prepared via nanosphere lithography and reactive ion etching, over soft substrates	up to ca.185	———	1350
PEDOT:PSS	SWNT(15%)	Wet-spinning and post-treatment	14000	0.064	1200
PEDOT:PSS	SWNT(95%)	Liquid-phase exfoliation	15	4000	90
PANI	SWNT(64%)	Solution mixing	47.8	769	176
PPy	GNPs(40%)	In suti chemical polymerization	31.74	101.68	10.24
PVAc	CNTs(20wt%)	Segregated network	80	48	30.7

Figure 4: Materials for modeling

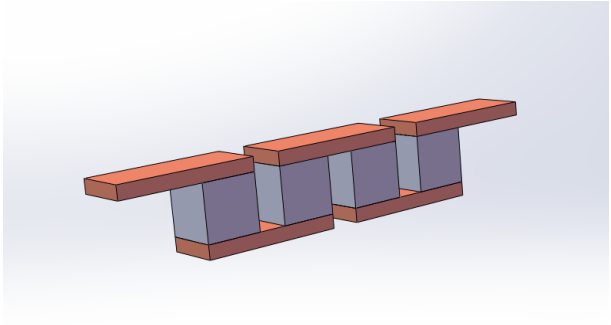

Figure 5: Physical model

electrodes are hot end and cold end respectively: then the directional migration of the carrier in the P-junction and N-junction occurs, and an electric potential difference is formed. Continuous power output is obtained if the electronic device and the battery are connected together to complete the circuit.

5.3 Simulation

The three-dimensional physical model of thermoelectric materials was established in COMSOL, and a steady-state model was realized. The model structure is composed of two basic battery units in series. The electrode material is copper, and the material of the P-junction and N-junction is bismuth telluride. Details of the material parameters can be seen in Table 1. The lower boundary condition of the material was set to a constant temperature. Considering that the thermoelectric material is used for the power supply of human wearable devices, the constant temperature was set to the skin temperature of the human body of 33 ℃[5]. The upper boundary condition of the material was also set to a constant temperature, which represented the ambient temperature. Considering the influence of different seasons, the variation range of the ambient temperature was 5-30 ℃. There are 6 conditions with an interval of 5 ℃. The other interfaces were set as thermal insulation. In addition, the initial current value of all the interfaces was set to 0 V. The battery model was divided into a regular hexahedron. There are 56 grid nodes, and 1896 grid cells, and the minimum grid quality is 0.997, which is very close to 1. The model calculation traverses 6 conditions.

Table 1: Physical parameters of model materials

Material	Heat capacity $[J/(kg \cdot K)]$	Density $[kg/m^3]$	Electric conductivity $[S/m]$	Thermal conductivity $[W/(m \cdot K)]$
Copper	385	8960	5.998×10^{-7}	400
Bi_2Te_3	154	7700	sigma(T)	k(T)

The results showed that the temperature in the battery decreased linearly from the hot end to the cold end. Due to the different temperature difference between the two ends, the temperature change rate was different, from 14×10^3 K/m to 1.5×10^3 K/m. According to the Peltier effect, different temperatures at both ends of the metal will generate current. This study found that the temperature difference between the cold and hot ends will affect the potential of the battery. The greater the temperature difference, the greater the potential energy generated (Figure 6). When the maximum temperature difference is 28 ℃, the corresponding potential difference is 23.21 mV; when the minimum temperature difference is 3 ℃, the corresponding potential difference is 2.54 mV. Two probes along the X-axis direction were designed to compare the electric potential and it was found that from probe 1 (-2, 1, 0.8) to probe 2 (13.6, 1, 0.8), with the decrease of the temperature difference between the cold and hot ends, the potential difference between the two probes also decreased.

However, this seems to be unfavorable for the design of wearable devices. Under the same power supply demand of an artificial heart, the potential difference of battery per unit mass is larger in winter and relatively small in summer. Therefore, the area of thermoelectric materials required increases in summer, and the area of clothing increases, which may be detrimental to human thermal comfort and

heat dissipation. An auxiliary power supply needs to be be matched when thermal power generation is not guaranteed in summer.

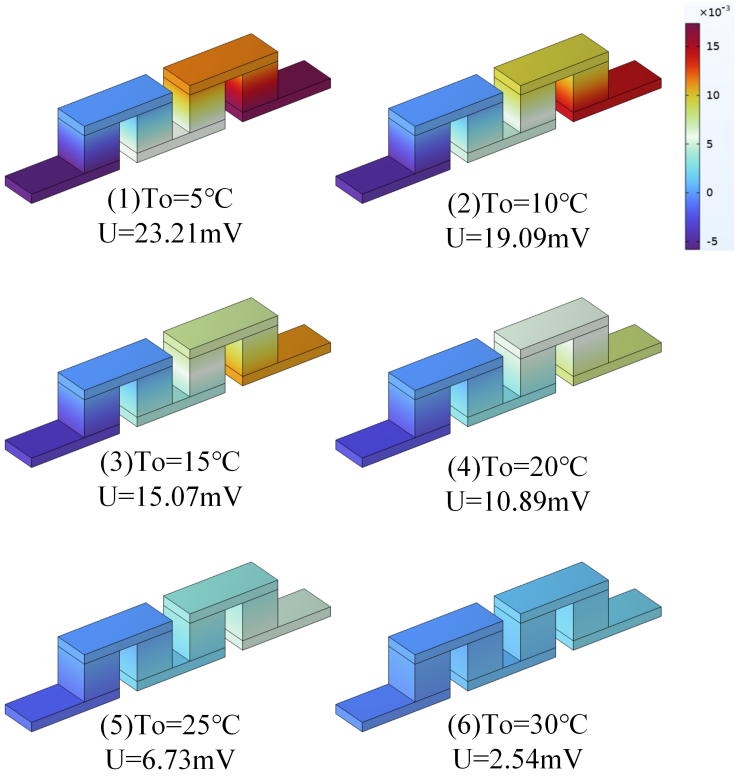

Figure 6: The electric potential field in different conditions

5.4 Different materials

Our team members provided seven relatively new thermoelectric materials. The data included some Seebeck coefficients, electric conductivity, ZT, and power factor treatment. For the COMSOL model deployed, we lacked more Seebeck coefficients at different temperatures. There were three ways to compensate.

First, we used the available material database in the Material Project to find the required materials. Although it is difficult to enter the chemical formula of certain materials, in this database it is possible to use the Material ID to retrieve specific materials, and ChatGPT was used to help in this regard. In this way, the heat capacity at constant pressure and density of materials were collected. Next, there is a Seebeck coefficient prediction model based on ML[6]. This takes the Seebeck coefficient of crystal materials in a temperature range of 300 K to 1000 K as the target property, and using the mechanical forest method establishes a model of 452 characteristic parameters including the basic physical properties of the constituent elements. In our program, we only took properties at room temperature into consideration, so we selected the data resulting from 300 K alone. The main method

of collecting data remained searches in literature databases such as Web of Science. The properties required for specific materials could be found through a keyword search. Image processing software was also used to obtain data that are not indicated in the chart but are valuable. We obtained 3-5 data points of Seebeck coefficient and electric conductivity under 0-300K[7] [8] [9] [10] [11].

After collecting the data, we used an interpolation method to fit the change function of relevant parameters with temperature in COMSOL. Finally,we generated some some data as seen below.

Materials	PEDOT/Bi2Te3	PANI/64%SWNT	PEDOT:PSS/SWNT60%	PPy/GNPs	PVAc/CNTs	PEDOT/CuCl2
$\Delta U/mV$	0.024	0.0313	0.00754	0.0223	0.0482	0.723

Figure 7: Electric potential of different materials

5.5 Limitations

In our resulting program, there are some differences from what we planned at first.

First, because of limited time, we were unable to establish a database of thermoelectric materials according to our objectives. This meant that we failed to do any work on building and training a machine learning model of our own. We were only able to use existing models to establish some of the parameters.

Second, we had limited access to many databases, so we could only find the data in databases such as the Web of Science. This made our work complex and time-consuming. Meanwhile, as we have show above, many important data concerning certain new materials are missing.

For these two reasons, we could only focus on 7 materials and simulate their performance in a certain application scenario. It was impossible to compare different materials in this case. At the same time, we were able to learn from many references that the combinations of different n-type materials and p-type materials can improve the efficiency. But in our model, we only chose some of them, and it is a limitation that perhaps some materials can only work as n-type or p-type materials. Then, apart from the inner part of the battery, we were forced to ignore the influence of electrode materials. Given more time and more data, electrode materials need be taken into consideration.

Author Contributions

Conceptualization:Z.Z.,S.G.,Y.Z. and J.Z;methodology,validation,formal analysis:Z.Z.,S.G.,Y.Z. and J.Z.;investigation,resources,data curation:Z.Z.,Y.Z. and J.Z.;writing-original draft preparation, visualization:S.G. and Z.Z.;writing-reviewing and editing, visualization and supervision:Y.Z and J.Z.;Project administration:Z.Z.,S.G. and Y.Z..All authors have read and agreed to the published version of the manuscript.

Funding

This research received no external funding.

Research Guidelines

This study followed the research guidelines of the Sustainable Energy and Battery Technology, Cambridge Academic Program (online) 2023.

Informed Consent Statement

Not Applicable.

Data Availability

Please contact the corresponding author(s) for all reasonable requests for access to the data.

Acknowledgments

We would like to give our thanks to our faculty professors and teachers at Cambridge University for their guidance.

Conflicts of Interest

The authors declare no conflict of interest.

Intellectual Property

The authors attest that copyright belongs to them, the article has not been published elsewhere, and there is no infringement of any intellectual property rights as far as they are aware.

References

[1] HJ Van Daal, PB Van Aken, and KHJ Buschow. The seebeck coefficient of ybal2 and ybal3. *Physics letters A*, 49(3):246–248, 1974. 2

[2] Raziel Riemer and Amir Shapiro. Biomechanical energy harvesting from human motion: theory, state of the art, design guidelines, and future directions. *Journal of neuroengineering and rehabilitation*, 8:1–13, 2011. 2

[3] Daniel Champier. Thermoelectric generators: A review of applications. *Energy Conversion and Management*, 140:167–181, 2017. 2

[4] Hussam Jouhara, Alina Żabnieńska-Góra, Navid Khordehgah, Qusay Doraghi, Lujean Ahmad, Les Norman, Brian Axcell, Luiz Wrobel, and Sheng Dai. Thermoelectric generator (teg) technologies and applications. *International Journal of Thermofluids*, 9:100063, 2021. 2

[5] Dengjia Wang, Guixia Chen, Cong Song, Yanfeng Liu, Wenfang He, Tingting Zeng, and Jiaping Liu. Experimental study on coupling effect of indoor air temperature and radiant temperature on human thermal comfort in non-uniform thermal environment. *Building and Environment*, 165:106387, 2019. 5.3

[6] Al'Ona Furmanchuk, James E. Saal, Jeff W. Doak, Gregory B. Olson, Alok Choudhary, and Ankit Agrawal. Prediction of seebeck coefficient for compounds without restriction to fixed stoichiometry: A machine learning approach. *Journal of Computational Chemistry*, 2018. 5.4

[7] L. Wang, F. Liu, C. Jin, T. Zhang, and Q. Yin. Preparation of polypyrrole/graphene nanosheets composites with enhanced thermoelectric properties. *Rsc Advances*, 4(86):46187–46193, 2014. 5.4

[8] J. Ha, J. Cho, S. Yoon, M. S. Jang, Syed Zahid Hassan, Min Gyun Kang, and D. S. Chung. Polyvinyl alcohol covalently grafted cnt for free-standing, flexible, and high-performance thermoelectric generator film. *Nanotechnology*, 2019. 5.4

[9] Siqi Liu, Hui Li, and Chaobin He. Simultaneous enhancement of electrical conductivity and seebeck coefficient in organic thermoelectric swnt/pedot: Pss nanocomposites. *Carbon*, 149:25–32, 2019. 5.4

[10] Q. Yao, Q. Wang, L. Wang, and L. Chen. Abnormally enhanced thermoelectric transport properties of swnt/pani hybrid films by the strengthened pani molecular ordering. *Energy Environmental Science*, 7(11):3801–3807, 2014. 5.4

[11] B. Kim, J. U. Hwang, and E. Kim. Chloride transport in conductive polymer films for an n-type thermoelectric platform. *Energy Environmental Science*, 13, 2020. 5.4